PCCP

Accepted Manuscript

ROYAL SOCIETY OF CHEMISTRY

www.rsc.org/pccp

Journal Name

ARTICLE

Nanoscale Characterization Illustrates the Cisplatin-Mediated the Biomechanical Changes of B16-F10 Melanoma Cells

Received 00th January 20xx,
Accepted 00th January 20xx

DOI: 10.1039/x0xx00000x

www.rsc.org/

Mei-Lang Kung[a], Chiung-Wen Hsieh[a], Ming-Hong Tai[b,c,d,g], Chien-Hui Weng[b], Deng-Chyang Wu[e,f,g,h], Wen-Jeng Wu[g,i,j,k,l], Bi-Wen Yeh[g,j,k], Shu-Ling Hsieh [m], Chao-Hung Kuo[e,g,n], Huey-Shan Hung[o,p] and Shuchen Hsieh[a,g,q*]

Cells reorganize their membrane biomechanical dynamics in response to environmental stimuli or inhibitors associated with their physiological/pathological processes, and disease therapeutics. To validate the biophysical dynamics during cells exposure to anti-cancer drugs, we investigate the nanoscale biological characterizations in melanoma cells undergoing cisplatin treatment. Using atomic force microscopy, we demonstrate that the cellular morphology and membrane ultrastructure are altered after exposure to cisplatin. In contrast to their normal spindle-like shape, cisplatin causes cell deformation rendering cells flat and enlarged, which increases the cell area by 3–4 fold. Additionally, cisplatin decreases the topography height values for both the cytoplasmic and nuclear regions (by 40–80% and 60%, respectively). Furthermore, cisplatin increases the cytoplasmic root mean square roughness by 110–240% in correlation with the drug concentration and attenuates the nuclear RMS by 60%. Moreover, the cellular adhesion force was enhanced, while the Young's modulus elasticity was attenuated by ~2 and ~2.3 fold, respectively. F-actin phalloidin staining revealed that cisplatin enlarges the cell size through enhanced stress fiber formation and promotes cytoskeletal reorganization. Immunoblot analyses further revealed that the activities of focal adhesion proteins, such as FAK and c-Src, are upregulated by cisplatin through phosphorylation at tyrosine 397 and 530, respectively. Collectively, these results show that cisplatin-treated melanoma cells not only exhibit upregulation of FAK-mediated signaling to enhance the cytoskeleton mechanical stretch, but also promote cytoskeletal rearrangement resulting in a 43% decrease in the cell modulus. These mechanisms thus promote malignancy and invasiveness of the melanoma cells.

[a] Department of Chemistry, National Sun Yat-sen University, 70 Lien-hai Rd., Kaohsiung 80424, Taiwan
[b] Department of Biological Sciences, National Sun Yat-Sen University, Kaohsiung 80424, Taiwan
[c] Institute of Biomedical Sciences, National Sun Yat-sen University, Kaohsiung 80424, Taiwan
[d] Center for Neuroscience, National Sun Yat-Sen University, Kaohsiung 80424, Taiwan
[e] Division of Gastroenterology, Department of Internal Medicine, Kaohsiung Medical University Hospital, Kaohsiung 80708, Taiwan
[f] Department of Medicine, College of Medicine, Kaohsiung Medical University, Kaohsiung 80708, Taiwan
[g] Center for Stem Cell Research, Kaohsiung Medical University, Kaohsiung 80708, Taiwan
[h] Department of Internal Medicine, Kaohsiung Municipal Ta-Tung Hospital, Kaohsiung 80708, Taiwan
[i] Graduate Institute of Medicine, College of Medicine, Kaohsiung Medical University, Kaohsiung 80708, Taiwan
[j] Department of Urology, Kaohsiung Medical University Hospital, Kaohsiung Medical University Kaohsiung 80708, Taiwan
[k] Department of Urology, School of Medicine, College of Medicine, Kaohsiung Medical University, Kaohsiung 80708, Taiwan
[l] Department of Urology, Kaohsiung Municipal Ta-Tung Hospital, Kaohsiung Medical University, Kaohsiung 80708, Taiwan
[m] Department of Seafood Science, National Kaohsiung Marine University, Kaohsiung 80811, Taiwan
[n] Department of Internal medicine, College of Medicine, Kaohsiung Medical University, Kaohsiung 80708, Taiwan
[o] Graduate Institute of Basic Medical Science, China Medical University, Taichung 40402, Taiwan
[p] Center for Neuropsychiatry, China Medical University Hospital, Taichung 40402, Taiwan
[q] School of Pharmacy, College of Pharmacy, Kaohsiung Medical University, Kaohsiung 80708,Taiwan

1. Introduction

The goals of chemo- and radiotherapy are to inhibit the growth of tumor cells, retard tumor progression, and increase the patient's survival period. However, conventional therapeutics faces several challenges. For instance, some tumor cells are resistant to drugs and acquire senescence instead. Cisplatin, a cell-cycle specific drug, is a first-line agent for several cancer therapeutics (either alone or in combination with other anticancer agents) including those for the ovary, testes, head and neck,[1] and melanoma.[2] The cytotoxicity of cisplatin results from its platinum-DNA adducts that inhibit efficient DNA replication and transcription. However, the antitumor efficiency of cisplatin is attenuated because of its dose-dependent nephro- and neurotoxicity, as well as intrinsic or acquired cellular resistance.[3] Recent reports have demonstrated the mechanisms of cisplatin resistance. These include exploiting efflux transporters,[4] deregulating signal transduction pathways and DNA damage-mediated apoptotic signals, enhancing DNA repair, and tolerating DNA damage.[3, 5-7] However, the effects of cisplatin on cellular mechanical properties are poorly understood.

Cellular mechanical properties are associated with many human physiological/pathophysiological processes including diseases (such as cancer) and tumorigenesis.[8-10] Unprecedented advances in computational biology and biomechanics[11] have now enabled researchers to probe the

mechanical responses of cells (and their constituents) to such processes, with significant implications in biotechnology and human health.[11] Cellular biomechanical properties are strongly influenced by the cytoskeleton, whose dynamic remodeling is involved in cell migration, adhesion, proliferation, differentiation,[12] and mechanotransduction. Therefore, altered cellular functions, induced by exogenous stimuli or inhibitors, can markedly remodel cellular biomechanical properties. For example, it is reported that stimulation of endothelial cells with tumor necrosis factor (TNF)-α significantly increases mechanical stiffness as well as the density of F-actin filaments.[13]. Further, altered cellular biophysical dynamics and ion channel activities along with elevated stiffness were observed upon glucose-mediated upregulation of intracellular Ca^{2+} levels in a pancreatic β-cell line.[14] Human pterygium fibroblast cells treated with the antimitotic mitomycin C also showed modified membrane surface topography and rigidity, which led to disturbed intracellular Ca^{2+} homeostasis and cytotoxicity.[15] Hence, drug treatments not only cause morphological and functional alterations in cells, but also result in their abnormal physical and structural dynamics. Currently, little is known about how chemotherapeutic drugs contribute to changes in the biomechanical properties of tumor cells. Advances in systemic therapies against malignant progression, such as for melanoma, have recently been reviewed. These include surgical and targeted therapy, cytotoxic chemotherapy, and tumor immunotherapy.[16] Melanoma is a malignant cancer with high mortality and a low survival rate, and is difficult to treat because of its pronounced drug-resistant characteristics.[17] Current research on anticancer drugs chiefly focuses on the molecular, immunological, and pathological,[18, 19] rather than mechanical aspects, where the latter might be pivotal to the pathophysiological outcomes.

Atomic force microscopy (AFM) is a high-resolution imaging technique widely applied in nanoscale biological characterizations.[11, 20] This technique offers several advantages: (1) provides information on the three-dimensional cellular topography and biophysical dynamics of cells undergoing various treatments;[14, 21](2) monitors the precise forces (at the level of piconewtons (pN)) in dynamic cellular processes such as deformation and cytoskeletal rearrangements, growth, exocytosis, and endocytosis;[22, 23] and (3) simultaneously records topographical and viscoelastic properties.[24]. These features allow elucidation of the differences between malignant and non-malignant cells even in the early pathological stages, where other methods might fail to detect them.[25-27]

Cisplatin is the most potent and popular chemotherapeutic agent for the treatment of various malignant tumors, including melanoma. In this study, we have used AFM to investigate the cytoskeletal rearrangements induced by cisplatin in the murine B16-F10 melanoma cell line. These biophysical properties include cellular size, height dynamics, surface roughness, adhesion forces, and stiffness. Moreover, we also demonstrate that the altered biomechanical properties are associated with upregulation of the FAK-Src focal adhesion signaling pathway, which is related to cytoskeletal mechanical stretch, cell survival, and invasiveness. Our study thus provides new insights into the mechanisms underlying cisplatin-resistance in melanoma cells and the associated metastasis.

2. Experimental

2.1 Drugs

Cisplatin [*cis*-diammineplatinum (II) dichloride] was purchased from Sigma-Aldrich (St. Louis, MO, USA) and dissolved in 0.15 M NaCl as indicated on the datasheet. Aliquots were stored at -20°C and thawed immediately before use.

2.2 Cell Culture

The murine B16-F10 melanoma cells were maintained in DMEM (GIBCO™) supplemented with 10% fetal bovine serum (HyClone, Thermo Scientific), 2 mM glutamine, 10 μg/mL streptomycin, and 100 U/mL penicillin at 37°C and 5% CO_2.

2.3 Atomic Force Microscopy (AFM)

Cells (5×10^4 cells/mL) were seeded on cover slides in 12 well culture plates (1 mL/well) overnight and then treated with cisplatin (0, 3, 5, and 10 μM) for 48 h at 37°C and 5% CO_2. For AFM imaging, attached culture slices were taken out and washed three times with phosphate-buffered saline (PBS, pH 7.4), fixed with 4% paraformaldehyde for 20 min, washed three times with PBS and then changed to ultra-pure water. An atomic force microscope (MFP-3D™, Asylum Research, Santa Barbara, CA) was used to characterize the cells under ambient conditions.[28] A silicon cantilever (NanoWorld, Switzerland, Arrow FMR) that had a measured spring constant of 2.8 N/m was used for imaging the melanoma cells. Images were collected in air using contact mode at a scan rate of 1 Hz. To collect force measurement data in the untreated and treated melanoma cells, a silicon nitride probe (NanoWorld, Switzerland, PNP-TR) that had a measured spring constant of 0.05 N/m was used. The force measurement experiments were conducted in PBS at am approach/retract rate of 0.2 Hz. The spring constants for both the cantilevers were determined using the thermal noise calibration method.[29]

2.4 Analysis of AFM Force Curves

Adhesion measurements were used to determine the cellular adhesion force, and were collected under liquid condition. The forces were measured either at specific points, or by using a force map array, and analyzed using the data analysis tools of the AFM software (Igor pro 6.36). By collecting force curves on the cell surface from untreated and cisplatin-treated cells respectively, the mechanical properties including hardness and modulus were be probed, and the cellular adhesion force can be acquired through pulling measurements. Further, we analyzed these force curves and the elastic properties of the sample can be extracted using the Hertzian contact model.[30, 31]. The Young's modulus of the surface can be obtained by analyzing the AFM force curves. The detail procedures used here has been described and characterized as our previously studies.[28, 32]

2.5 Immunofluorescence

To examine the cytoskeleton, cells were treated with cisplatin (3 μM) for 48 h, and after two ice-cold PBS washes, they were fixated with 4% paraformaldehyde. Next, the cells were permeabilized with 0.2% Triton X-100 (Sigma–Aldrich) and incubated with Alexa Fluor 488-phalloidin (Invitrogen) for 15 min. The nuclei were stained with DAPI (Sigma-Aldrich). The confocal images were captured on a Zeiss LSM 510 inverted laser-scanning fluorescence microscope equipped with LSM 510 acquisition software, using a ×63 oil-immersion objective. Green fluorescence was acquired at 505-530 nm with an excitation at 488 nm. The fluorescence images were processed with Adobe Photoshop 9.0.

2.6 Western Blot Analysis

To detect the effect of cisplatin on cellular adhesion, the B16-F10 melanoma cells were treated with various concentrations of cisplatin (0.1, 1, 3, 5, and 10 μM) for 48 h. They were then harvested and subjected to western blot analysis. Protein extracts were prepared using RIPA buffer [150 mM NaCl, 50 mM HEPES (pH 7.0), 1% Triton X-100, 10% glycerol, 1.5 mM $MgCl_2$, 1 mM EGTA, and protease inhibitors (Roche Applied Science)]. The protein extracts (20 μg) were subjected to SDS-PAGE and transferred onto PVDF membranes (Pall Corporation). Next, the membranes were incubated with primary antibodies including rabbit anti-phospho-FAK (Y397) (Cell Signaling Technology, Inc.), rabbit anti-FAK, mouse anti-phospho-c-Src (Y530), and mouse anti-c-Src (Santa Cruz Biotechnology). The immunoreactive signals were visualized by using the Immobilon Western Chemiluminescent HRP Substrate (Millipore).

2.7 Statistical Methods

The root-mean-square (RMS) roughness data of the cytoplasmic and nuclear surfaces of three cells were acquired and analyzed using AFM. Western blots were performed at least three times. Data are represented as mean ± standard error of the mean (SEM) of indicated experiments. A P value <0.05 obtained by paired Student's *t*-test was considered statistically significant.

3. Results and discussion

3.1 Cisplatin-mediated Alteration of Cytoplasmic and Nuclear Biophysical Structures Affects Cellular Size Deformation

Three anti-proliferative responses induced by chemotherapy i.e., apoptosis, mitotic catastrophe, and senescence, are well investigated.[33] However, the effects on the membrane biophysical properties are still unclear. To validate such effects of cisplatin, the melanoma B16-F10 cells were treated with various concentrations of the drug (3, 5, and 10 μM) for 48 h, and the morphologies of the surviving cells were monitored by microscopy and AFM. Fig. 1 shows that the sizes of these cells were increased and their bodies deformed, appearing flat and spread over the surface. Further, these deformations were more obvious with increasing concentrations of cisplatin, compared with that in the control cells (with spindle-like morphology) (Fig. 1A and 1B-(i)). Additionally, the AFM topological images (Fig. 1B-(ii)) show that cisplatin enlarges

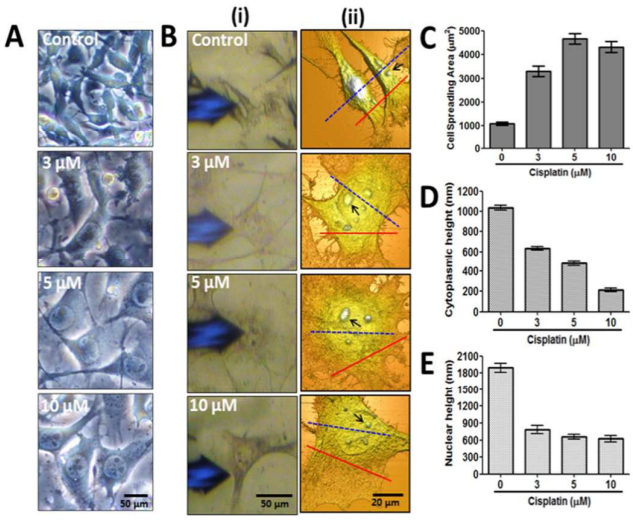

Fig. 1 Cisplatin induces morphological changes in B16-F10 melanoma cells. (A) Microscopy images of the cells treated with various doses of cisplatin (0, 3, 5, and 10 μM) for 48 h showing cisplatin-mediated cellular morphological and size changes in a dose-dependent manner. (B) (i) Bright field optical images acquired with the AFM system showing the probe tip positioned near the cells of interest prior to AFM scanning. (ii) Topological images (70 × 70 □m^2) showing the size and detailed structure of the cells (black arrows indicate the nucleolus positions). (C) Quantification showing the cisplatin-mediated increase in cell area (cell numbers, n = 12). (D) AFM topographical images reveal a decrease in cytoplasmic height with increasing cisplatin concentration. (E) Nuclear height values showing a decrease in the mean value (689 ± 139 nm) compared with the control group (1895 ± 192.5 nm). The height values of cytoplasmic heights and nuclear heights were obtained from (ii) red and blue-dashed cross-sections lines, respectively. The bar represents mean ± S.D. ** p <0.005.

the boundary of the cell body as well as the nuclear dimensions and shows manifest nucleoli (black arrow) within the nuclear region compared with the untreated cells. Alterations observed in the intracellular biomechanical structures include increase in the roughness and granularity of the cytoplasm at 3, 5, and 10 μM cisplatin. The number of nucleoli was also increased in presence of cisplatin compared to the untreated cells (3–5 vs. 2–3 nucleoli, respectively). We further evaluated the cell areas following cisplatin treatment. The data shows that the areas of the treated cells were 1097 ± 217, 3300 ± 697, 4674 ± 679, and 4326 ± 697 μm^2 at 0, 3, 5, and 10 μM cisplatin, respectively (Figure 1C). These results suggest that cells might deform their morphologies and dimensions, and modify their mechanical properties in response to cisplatin-mediated death. Next, we characterized the biomechanical dynamic effects of cisplatin on the melanoma cells. Cells were imaged using AFM to validate the cellular topography heights of the cytoplasmic and nuclear regions. Fig. 1D illustrates that cisplatin elicits a significant dose-dependent decrease in cytoplasmic height with a quantification of 1,035 ± 63.5, 633 ± 40.2, 476 ± 51.6, and 215 ± 39.7 nm at 0, 3, 5, and 10 μM of cisplatin, respectively. Interestingly, cisplatin also dramatically decreased the nuclear height with a

quantification of 1,895 ± 192.5, 787 ± 180.7, 657 ± 94, and 622 ± 143.6 nm at 0, 3, 5, and 10 μM of cisplatin, respectively (Fig. 1E). These results indicate that cisplatin-elicited cellular dimensional changes occur through extending and deforming their cytoplasmic and nuclear mechanical structures.

To escape destruction by physical radiation or chemical agents, some tumor cells do not undergo an arrest in G1 and/or G2 phases and are either repaired or die by apoptosis. they re-enter the cell cycle and skip cell cycle checkpoints instead and generate newly born cancer cells.[34] Some natural compounds such as alkaloids and taxanes induce depolymerization and hyperpolymerization of microtubules, respectively. Both lead to cell enlargement, defects in the mitotic assembly, delayed mitosis, and microtubule disorders–characteristic of giant cells.[35, 36] Previous studies have demonstrated that the giant cell state is a way of escaping cell death.[37] Meanwhile, nucleoli are organelles involved in transcription, gene processing, and ribosomes biogenesis. Upon exposure to cytotoxic stimuli, nucleoli rapidly lose their compact organization, the nucleolar proteins delocalizing to the nucleoplasm. This impairs pre-ribosomal RNA (pre-rRNA) transcription. In this vein, hypertrophic and irregularly shaped nucleoli, both abnormal morphologies, have been associated with malignancy. Therefore, altered nucleolar numbers and sizes might contribute to neoplastic transformation and the genesis of cancer.[38, 39] Altogether, cisplatin induces intracellular cytoskeletal rearrangements such as the redistribution of microtubules and actin filaments[40, 41] that further alters the cytoplasmic and nuclear heights, mechanical dynamics, and promotes morphological deformation. Our results also indicate that cell enlargement is associated with a growth arrest mechanism to resist cisplatin and enter a pre-senescence state.

3.2 Cisplatin induces cellular membrane ultrastructures remodeling

Next, we examined the surface morphologies and ultrastructure of the cisplatin treated cells. Our results show that cisplatin gradually increased the cytoplasmic roughness and granularity in a dose-dependent manner (Fig. 2A), while the surface of the nuclear region became relatively smooth compared with that of the control cells (Fig. 2B). The membrane surface RMS roughness of the cytoplasmic region also reflected the dose-dependent increase (33 ± 2.8, 38 ± 3.1, 60 ± 4.2, and 78 ± 5.3 nm at 0, 3, 5, and 10 μM cisplatin treatment, respectively) (Fig. 2C). For the nuclear region, following cisplatin administration, the RMS roughness values revealed a downward trend (24 ± 5, 26 ± 4, and 26 ± 4.2 nm at 3, 5, and 10 μM cisplatin treatment, respectively) as compared to the control (37 ± 3.0 nm) (Fig. 2D). We further characterized the time effects of cisplatin treatment on cellular surface morphologies and ultrastructure. Our results reveal that cisplatin elicits an obvious increase in the cytoplasmic RMS and a decrease in the nuclear RMS in a time-dependent manner. In addition, we observed significant cisplatin-mediated RMS changes at 48 h of treatment. (Fig. S1). Altogether, these results suggest that cisplatin induces cellular ultrastructure changes in a dose- and time-dependent manner. Moreover, the cisplatin-mediated cytoplasmic roughness might be associated with microtubule disassembly and the induction of a porous appearance.

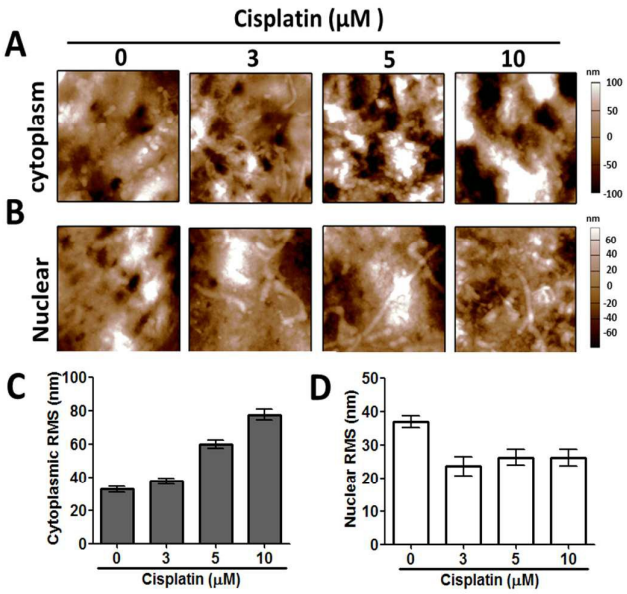

Fig. 2 Effects of cisplatin on the nuclear and cytoplasmic surface roughness. After the B16-F10 cells were treated with various concentrations of cisplatin for 48 h, ultrastructures of the cytoplasm (A) and nucleus (B) were determined from the AFM topographical images. The changes in the RMS roughness of the cytoplasm (C) and nucleus (D) are shown. Image size in (A) and (B) is 5 × 5 μm^2. The height values were obtained from at least 10 cells and the bars in (C) and (D) represent the mean ± S.D.; p <0.005.

Cisplatin acts on tumor cells by inducing cytotoxicity, generating mutagenic DNA adducts, interfering with DNA/RNA synthesis and disturbing microtubule function during cell division.[42] Previous studies have reported that cytotoxic anti-cancer drugs like colchicine and cytarabine also increase roughness in HeLa, HepG2, and C6 cell lines. They also suggest that drug-mediated microtubule depolymerization is involved in the membrane ultrastructure change.[25] Additionally, accumulating studies demonstrate that cisplatin targets not only DNA, but also intracellular lesions that cause structural alterations of cellular organelles and cytoskeletal components such as microtubules, intermediate filaments, and microfilaments. Cisplatin alters microtubule assembly by direct tubulin modification via binding to GTP in the GTP center of tubulin. Therefore, these additional interactions fortify the anti-proliferative effect, contributing to growth inhibition and giant cell formation.[40, 41, 43] Moreover, the relationship between cellular surface roughness and tumor malignancy has been demonstrated. Various grades of human breast cancer have been used to study the surface topology. It was observed that normal breast tissue has a smoother surface topography, and with increasing stages of cancer (from Grade I to Grade III), elevation of surface roughness occurred. [44] In this study, the enlarged cell size, decreased cellular height (Fig. 1) and increased cytoplasmic roughness and granularity (Fig. 2) are associated with the cisplatin-mediated structural alterations of cellular organelles, and disturbed cytoskeletal components. These results also reveal that cisplatin-enlarged melanoma cells may possess the potential for drug resistance and malignancy.

3.3 Analysis of Biophysical Dynamics of Cisplatin-treated Cells: Cellular Adhesion Force and Young's Modulus Elasticity

To delve deeper into the effects of cisplatin on the biomechanical properties of cells, we measured the cell adhesion force and cell modulus. Toward this aim, cells were incubated with or without cisplatin (3 μM) for 48 h and then AFM measurements were performed. As shown in Fig. 3, the AFM topographical images were subsequently used as a map of the cell surfaces, over which we acquired and analyzed an array of force curves to determine the adhesion force and Young's modulus (elasticity) at each point in the array. A total of 225 and 587 points on the untreated (Fig. 3A) and cisplatin-treated (Fig. 3B) cells, respectively, were collected and analyzed. The locations of the individual force curves are represented on the cell images as a 32 × 32 μm^2 grid. In each grid, the squares measured to be >80 (red) and <80 kPa (blue) reveal that cisplatin increases the cellular adhesion force in contrast to the controls (peaking at 69.2 ± 18 and 33.2 ± 15 pN, respectively) (Fig. 3C). In addition, the nanomechanical signatures and elasticity maps (Fig. 3D) obtained for the control group (gray) showed an average Young's modulus of 124 ± 35 kPa. In contrast, elasticity maps recorded for the cisplatin group (blue) showed an average Young's modulus of 53 ± 21 kPa. The cisplatin-treated cells appeared 43% softer compared to the control cells. These results indicate that cisplatin-treated cells exhibit greater adhesion force and lesser stiffness.

This might arise from: (1) alterations in membrane lipid components, (2) altered membrane fluidity, and/or (3) cytoskeleton rearrangement at the inner surface of the membrane. Recently, Cross et al.[26] showed that cancer cell stiffness is strongly correlated with deformability and malignancy. Previous studies have also indicated that altered cell stiffness (usually becoming softer) is associated with tumor progression both *in vivo* [26] and *in vitro* [10, 45]. And, recent work by Fletcher et al. [46] has demonstrated that both internal and external physical forces can act on the cytoskeleton to affect local mechanical properties and cellular behavior. Our results suggest that cisplatin enhances cellular adhesion force and decreases cell stiffness which may be associated with tumor cell malignancy and drug resistance.

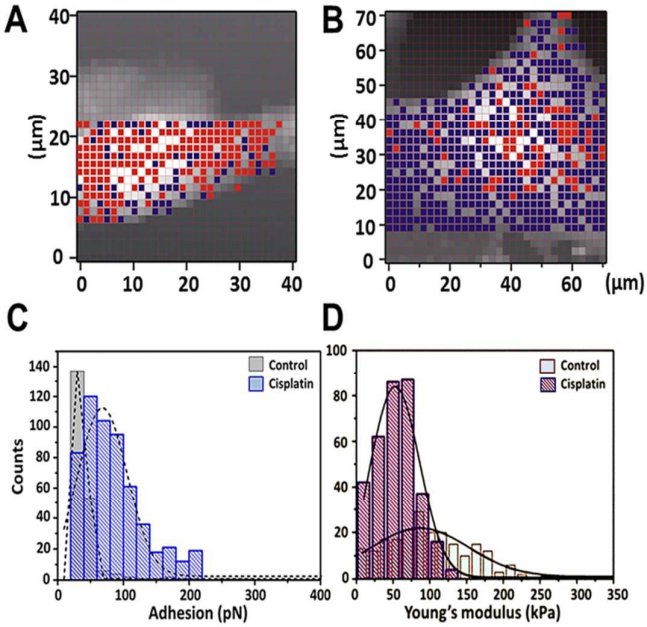

Fig. 3 Analysis of adhesion forces and the Young's modulus in cisplatin-treated melanoma cells. Cells were incubated with or without cisplatin (3 μM) for 48 h. Force maps were generated using AFM and the resulting topography data is shown for un-treated (A) and cisplatin-treated (B) cells (40 × 40 and 70 × 70 μm^2, respectively). Adhesion forces and elasticity were calculated from the force map data for each cell in the areas indicated by the color overlays shown in (A) and (B). (C) Histogram of **adhesion force** values from the force maps for untreated (gray-dashed) and cisplatin-treated cells (blue-dashed), showing average values of 33.2 ± 15 and 69.2 ± 18 pN, respectively. (D) Histogram of the **Young's modulus** values calculated from each force curve in the force map data array, showing average values of 124 ± 35 and 53±21 kPa for untreated (white-solid) and cisplatin-treated cells (purple-solid), respectively. Red squares (■) in the topography data overlay correspond to elastic modulus values >80 kPa, while blue ones (■) correspond to those <80 kPa.

3.4 Activation of Biomolecular Signaling in Response to Cisplatin-mediated Cytoskeleton Mechanotransduction

Focal adhesion requires integrins, and cytoskeletal and signalling proteins such as FAK and Src. These are sites for cytoskeletal contact with the extracellular matrix (ECM), which is essential for maintenance of the cellular architecture and mechanical sensing of the environment.[47, 48] Cytoskeletal reorganization is important to the cells' ability to adapt to exogenous stimuli or inhibitors from the surrounding microenvironment.[45, 49] Therefore, signalling proteins related to this reorganization are pivotal in cellular morphogenesis and biophysical dynamics. To demonstrate the effects of cisplatin on cytoskeleton rearrangement, the B16-F10 cells were treated with cisplatin for 48 h, and F-actin phalloidin staining was performed. Fig. 4A shows that cisplatin induced lamellipodia and stress-fiber formation and extended the F-actin filaments to support the enlarged cells. Conversely, most of the control cells maintained their spindle-like morphologies and revealed a lesser amount of stress fibers. The drastically altered levels of F-actin filaments in the cisplatin-enlarged cells appear to influence lamellipodia generation, stress fibers formation and cell adhesions. All these events are intimately associated with the motile activity of the cell.[50] This result then led us to validate the expressions of the focal adhesion related proteins FAK and Src. Previous studies have indicated that FAK activation regulates the mechanical properties of cells and modulates cellular stiffness and contractile forces,[48], which further contribute to invasiveness and subsequently, metastasis. In this context, our results reveal that the FAK activation (autophosphorylation at Y397-FAK) was induced 1.4–4 fold in the cisplatin-treated cells with a dose-dependent manner (Fig. 4B). Subsequently, a downstream protein of the FAK-mediated signalling

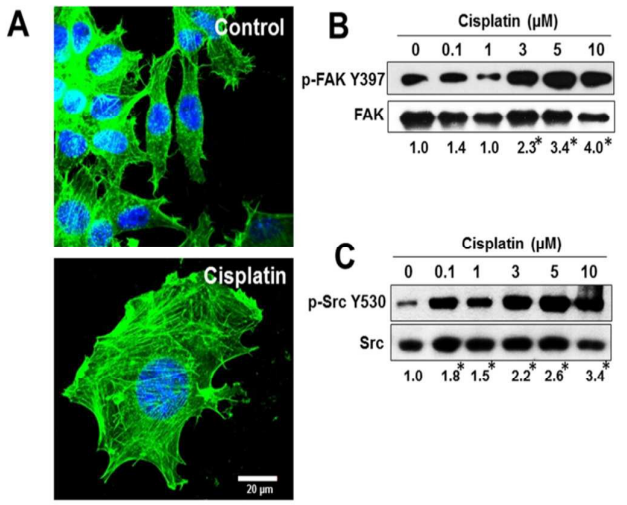

Fig. 4 Exposure of melanoma cells to cisplatin results in giant cell formation and FAK/Src signal activation. The B16-F10 cells were treated with cisplatin (3 μM) for 48 h, and subjected to phalloidin staining for actin filament detection. (A) Cisplatin exposure significantly increases cell size and F-actin stress fibers compared with the control group. (B and C) Cisplatin exposure activates cellular focal adhesion-related proteins FAK and Src in a dose-dependent manner. *p <0.01.

pathway, Src, was also activated (phosphorylation at Y530-Src) 1.5–3.4 fold in a dose-dependent manner (Fig. 4C). These results indicate that cisplatin alters the biomechanical properties not only reorganizing the F-actin filaments, but also activating the FAK-Src signalling pathway. Regulation of the cellular mechanical properties must be in accord with cell proliferation, morphogenesis, migration or invasion, and viability. This is important for various normal physiological processes such as immune response and wound healing; and pathological processes such as cancer cell invasion, metastasis, and drug resistance. For these reasons, coordination between the intracellular cytoskeletal dynamics and signal transductions is necessary. In this study, we found that cisplatin-enlarged cells reveal a rougher membrane surface (Fig. 2), lower young's modulus and higher adhesion force (Fig. 3) as well as inducing F-actin filaments reorganization and lamellipodia formation (Fig. 4) in the B16-F10 melanoma cells. The increased surface roughness and decreased cellular elasticity are associated with tumor progressiveness and has higher metastasis potential. [44, 45] Therefore, our results indicate that cisplatin-mediated loss of cell stiffness may increase the relative metastatic potential compared with the control.

The FAK-Src pathway can be activated by various signalling molecules that mediate proliferation, survival, cell adhesion, and invasion.[51, 52] Cowell et al. indicated that activation of Src/FAK/p130Cas/BCAR1 adhesion signalling during tamoxifen treatment in MCF-7 breast cancer cells may confer a survival advantage.[53] Moreover, upregulation of this pathway is also reported to be associated with cytoskeletal mechanical stretch.[48, 54] Interestingly, overexpression of FAK is documented to be involved in the invasiveness of malignant melanomas.[55] In this study, we found that cisplatin alters the melanoma cell morphology through increasing the cell size. It also alters the biomechanical properties by increasing the cellular adhesion forces and decreasing the Young's modulus of elasticity as well as promoting cytoskeletal reorganization and FAK-mediated signalling (Fig. 5) that are all involved in cell survival and malignancy. Therefore, the melanoma cells responds to cisplatin by the above mechanisms in order to escape from drug-induced cell death.

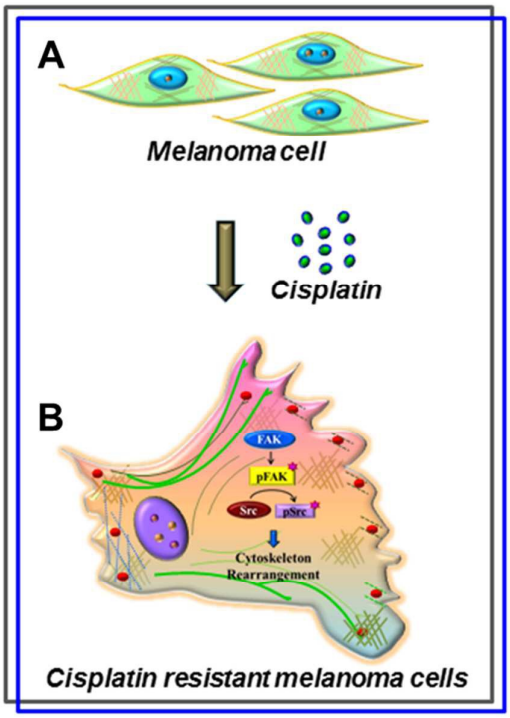

Fig.5 Alterations of biophysical structures, actin cytoskeletal dynamics and activation of focal contact signalling in cisplatin resistant B16-F10 melanoma cells. (A) The spindle-like B16-F10 cell regulates its cytoskeleton in a precise arrangement to maintain its architecture and morphology. (B) After cells were treated with cisplatin and acquired resistance, they responded immediately by changing their biomechanical properties such as increasing cell roughness and cell adhesion force, as well as decreasing the Young's modulus. Following alterations of biomechanical properties, FAK/Src focal adhesion signalling is activated resulting in cytoskeletonal reorganization and thereby reshaping the cellular architecture and morphology. This outcome may result in cell deformability, survival and cell invasiveness.

4. Conclusions

In summary, we utilized AFM technology for the first time to investigate the cisplatin-induced alterations in the morphology and ultrastructure of the B16-F10 melanoma cells. We determined high-resolution qualitative and quantitative changes in the texture of the cell surface, intracellular focal adhesion proteins, and cytoskeletal

rearrangements. Our results show that cisplatin alters the biophysical properties of cells by promoting their enlargement (Fig. 5). Based on high-resolution AFM images, we found that cisplatin attenuates cellular topography height and increases membrane roughness of the cytoplasmic region. Further, elevated cellular adhesion forces and decreased Young's modulus of elasticity indicate that cisplatin fosters softer cytoskeletal structure to promote deformability, cell survival and invasiveness. Our study therefore contributes to the potential diagnostic platforms for studying cell resistance based on their biomechanical dynamics and cytoskeletal organization signatures. The results might offer a therapeutic strategy for melanoma cell escape from cisplatin-mediated cytotoxicity and/or aid in the development of medicines useful against drugs resistant.

Acknowledgements

The authors would like to thank the Ministry of Science and Technology of Taiwan (NSC 104-2628-M-110-001-MY3), and Kaohsiung Medical University "Aim for the Top Universities Grant, KMU-TP104G00, KMU-TP104G01, KMU-TP104G03 and KMU-TP104G04, as well as the National Sun Yat-sen University Biochip Research Group for financial support of this work. Prof. Hsieh also thanks Dr. David Beck for helpful discussions.

Notes and references

1. A. W. Prestayko, J. C. D'Aoust, B. F. Issell and S. T. Crooke, *Cancer treatment reviews*, 1979, 6, 17-39.
2. A. Daponte, P. A. Ascierto, A. Gravina, M. Melucci, S. Scala, A. Ottaiano, E. Simeone, G. Palmieris and G. Comella, *Anticancer research*, 2005, 25, 1441-1447.
3. A. Basu and S. Krishnamurthy, *Journal of nucleic acids*, 2010, 2010.
4. A. R. Kirtane, S. M. Kalscheuer and J. Panyam, *Advanced drug delivery reviews*, 2013, 65, 1731-1747.
5. N. Kondo, A. Takahashi, K. Ono and T. Ohnishi, *Journal of nucleic acids*, 2010, 2010, 543531.
6. Z. H. Siddik, *Oncogene*, 2003, 22, 7265-7279.
7. L. Galluzzi, L. Senovilla, I. Vitale, J. Michels, I. Martins, O. Kepp, M. Castedo and G. Kroemer, *Oncogene*, 2012, 31, 1869-1883.
8. G. Y. Lee and C. T. Lim, *Trends in biotechnology*, 2007, 25, 111-118.
9. I. Titushkin and M. Cho, *Biophysical journal*, 2007, 93, 3693-3702.
10. S. Suresh, *Acta biomaterialia*, 2007, 3, 413-438.
11. G. Bao and S. Suresh, *Nature materials*, 2003, 2, 715-725.
12. S. Li, J. L. Guan and S. Chien, *Annual review of biomedical engineering*, 2005, 7, 105-150.
13. S. Y. Lee, A. M. Zaske, T. Novellino, D. Danila, M. Ferrari, J. Conyers and P. Decuzzi, *International journal of nanomedicine*, 2011, 6, 179-195.
14. R. Yang, N. Xi, K. W. Lai, K. C. Patterson, H. Chen, B. Song, C. Qu, B. Zhong and D. H. Wang, *Nanomedicine : nanotechnology, biology, and medicine*, 2013, 9, 636-645.
15. X. Cai, X. Yang, J. Cai, S. Wu and Q. Chen, *The journal of physical chemistry. B*, 2010, 114, 3833-3839.
16. M. Batus, S. Waheed, C. Ruby, L. Petersen, S. D. Bines and H. L. Kaufman, *American journal of clinical dermatology*, 2013, 14, 179-194.
17. E. Atallah and L. Flaherty, *Current treatment options in oncology*, 2005, 6, 185-193.
18. M. Vanneman and G. Dranoff, *Nature reviews. Cancer*, 2012, 12, 237-251.
19. C. Holohan, S. Van Schaeybroeck, D. B. Longley and P. G. Johnston, *Nature reviews. Cancer*, 2013, 13, 714-726.
20. Y. F. Dufrene, *Nature reviews. Microbiology*, 2004, 2, 451-460.
21. C. Peetla, S. Vijayaraghavalu and V. Labhasetwar, *Advanced drug delivery reviews*, 2013, 65, 1686-1698.
22. H. X. You, J. M. Lau, S. Zhang and L. Yu, *Ultramicroscopy*, 2000, 82, 297-305.
23. O. Chaudhuri, S. H. Parekh, W. A. Lam and D. A. Fletcher, *Nature methods*, 2009, 6, 383-387.
24. L. M. Rebelo, J. S. de Sousa, J. Mendes Filho and M. Radmacher, *Nanotechnology*, 2013, 24, 055102.
25. J. Wang, Z. Wan, W. Liu, L. Li, L. Ren, X. Wang, P. Sun, L. Ren, H. Zhao, Q. Tu, Z. Zhang, N. Song and L. Zhang, *Biosensors & bioelectronics*, 2009, 25, 721-727.
26. S. E. Cross, Y. S. Jin, J. Rao and J. K. Gimzewski, *Nature nanotechnology*, 2007, 2, 780-783.
27. G. Weder, M. C. Hendriks-Balk, R. Smajda, D. Rimoldi, M. Liley, H. Heinzelmann, A. Meister and A. Mariotti, *Nanomedicine : nanotechnology, biology, and medicine*, 2014, 10, 141-148.
28. S. Hsieh, P.-Y. Lin, C.-W. Hsieh, I. T. Li, S.-L. Hsieh, C.-C. Wu, Y.-S. Huang, H.-M. Wang, L.-W. Tu, K.-H. Cheng, H.-Y. J. Wang and D.-C. Wu, *Journal of the Chinese Chemical Society*, 2012, 59, 929-933.
29. J. L. Hutter and J. Bechhoefer, *Review of Scientific Instruments*, 1993, 64, 1868-1873.
30. S. Sen, S. Subramanian and D. E. Discher, *Biophysical journal*, 2005, 89, 3203-3213.
31. H. H., *J. Reine Angew. Math.*, 1882, 92.
32. S. Hsieh, I. T. Li, C.-W. Hsieh, M.-L. Kung, S.-L. Hsieh, D.-C. Wu, C.-H. Kuo, M.-H. Tai, H.-M. Wang, W.-J. Wu and B.-W. Yeh, *Arabian Journal of Chemistry*, DOI: 10.1016/j.arabjc.2015.08.011
33. I. B. Roninson, *Drug resistance updates : reviews and commentaries in antimicrobial and anticancer chemotherapy*, 2002, 5, 204-208.
34. R. Rajaraman, D. L. Guernsey, M. M. Rajaraman and S. R. Rajaraman, *Cancer cell international*, 2006, 6, 25.
35. H. Vakifahmetoglu, M. Olsson and B. Zhivotovsky, *Cell death and differentiation*, 2008, 15, 1153-1162.
36. R. Horbay and R. Stoika, *Central European Journal of Biology*, 2011, 6, 675-684.
37. L. L. Hall, J. P. Th'ng, X. W. Guo, R. L. Teplitz and E. M. Bradbury, *Cancer research*, 1996, 56, 3551-3559.
38. L. Montanaro, D. Trere and M. Derenzini, *The American journal of pathology*, 2008, 173, 301-310.
39. D. Avitabile, B. Bailey, C. T. Cottage, B. Sundararaman, A. Joyo, M. McGregor, N. Gude, S. Truffa, A. Zarrabi, M. Konstandin,

M. Khan, S. Mohsin, M. Völkers, H. Toko, M. Mason, Z. Cheng, S. Din, R. Alvarez, K. Fischer and M. A. Sussman, *Proceedings of the National Academy of Sciences*, 2011, 108, 6145-6150.
40. K. Boekelheide, M. E. Arcila and J. Eveleth, *Toxicology and applied pharmacology*, 1992, 116, 146-151.
41. P. Kopf-Maier and S. K. Muhlhausen, *Chemico-biological interactions*, 1992, 82, 295-316.
42. J. D. Maltzman and C. Vachani, *Abramson Cancer Center of the University of Pennsylvania.* , 2007.
43. A. A. Tulub and V. E. Stefanov, *International journal of biological macromolecules*, 2001, 28, 191-198.
44. R. Kaul-Ghanekar, S. Singh, H. Mamgain, A. Jalota-Badhwar, K. M. Paknikar and S. Chattopadhyay, *BMC cancer*, 2009, 9, 350.
45. W. Xu, R. Mezencev, B. Kim, L. Wang, J. McDonald and T. Sulchek, *PloS one*, 2012, 7, e46609.
46. D. A. Fletcher and R. D. Mullins, *Nature*, 2010, 463, 485-492.
47. P. P. Provenzano and P. J. Keely, *Journal of cell science*, 2011, 124, 1195-1205.
48. C. T. Mierke, *Physical biology*, 2013, 10, 065005.
49. M. Nikkhah, J. S. Strobl, R. De Vita and M. Agah, *Biomaterials*, 2010, 31, 4552-4561.
50. U. Lindberg, R. Karlsson, I. Lassing, C. E. Schutt and A. S. Hoglund, *Seminars in cancer biology*, 2008, 18, 2-11.
51. S. Li, W. Dong, Y. Zong, W. Yin, G. Jin, Q. Hu, X. Huang, W. Jiang and Z. C. Hua, *Molecular therapy : the journal of the American Society of Gene Therapy*, 2007, 15, 515-523.
52. V. M. Golubovskaya, *Anti-cancer agents in medicinal chemistry*, 2010, 10, 735-741.
53. L. N. Cowell, J. D. Graham, A. H. Bouton, C. L. Clarke and G. M. O'Neill, *Oncogene*, 2006, 25, 7597-7607.
54. B. Xu, G. Song, Y. Ju, X. Li, Y. Song and S. Watanabe, *Journal of Cellular Physiology*, 2012, 227, 2722-2729.
55. N. A. Chatzizacharias, G. P. Kouraklis and S. E. Theocharis, *Expert opinion on therapeutic targets*, 2007, 11, 1315-1328.